A solar cycle of cosmic-ray fluxes for 2006–2014: Comparison between PAMELA and neutron monitors

Sergey A. Koldobskiy[1, 2], Gennady A. Kovaltsov[3], Ilya G. Usoskin[1]

Ilya Usoskin, ilya.usoskin@oulu.fi

[1]University of Oulu, Finland.

[2]National Research Nuclear University "MEPhI", Moscow, Russia

[3]Ioffe Physical-Technical Institute, St. Petersburg, Russia.

This article has been accepted for publication and undergone full peer review but has not been through the copyediting, typesetting, pagination and proofreading process, which may lead to differences between this version and the Version of Record. Please cite this article as doi: 10.1029/2018JA025516

Abstract. A comparison of cosmic proton spectra directly measured by the PAMELA experiment during 2006–2014 with data of polar neutron monitors for the same time interval is presented. It is shown that the measured spectra are well described by the force-field model for the modulation potential range 350 – 750 MV. The obtained modulation potential agrees with that calculated from the data of the world neutron monitor network for low solar activity between 2006 and 2012 but diverges during the maximum of solar cycle. The empirical relation between the modulation potential and the (inverted) NM count rate appears somewhat steeper than the modelled one, as confirmed also by data from fragmentary balloon-borne measurements. A reason for the discrepancy is unclear and calls for additional study using independent datasets.

Keypoints:

- The GCR proton spectra measured by PAMELA are well described by the force-field model.
- PAMELA data is in good agreement with neutron monitors for low solar activity 2006–2012 but diverge for higher activity in 2013–2014.
- The systematic discrepancy is possibly related to an underestimate of the neutron monitor yield function in the high energy range.

1. Introduction

Galactic cosmic rays (GCR) depict a great deal of variability as measured near Earth, while their flux can be assumed constant outside the heliosphere. Thus, the flux of GCR near Earth serves as a probe for the large scale heliosphere and its changes, both cyclic and transient. The worldwide network of ground-based neutron monitors (NMs) is the main instrument to record GCR variability since 1951 [*Belov*, 2000; *Simpson*, 2000; *Shea and Smart*, 2000; *Bazilevskaya et al.*, 2014]. Because of the geomagnetic shielding, most sensitive are (sub)polar NMs located in regions with small geomagnetic rigidity cutoff. As an example, the variability of GCR recorded by a polar Oulu NM is shown in Figure 1 and depicts the dominant 11-year cyclic modulation as well as shorter noise-like transient changes. Since a NM detects not the primary GCR particles but secondary nucleonic component of the atmospheric cascade, it is not straightforward to relate the NM count rates to the GCR flux. A NM is an energy integrating instrument,which is most sensitive to the primary GCR with energy ranging between a few GeV to several tens of GeV. Sometimes it is assumed that NM count rate is linked to a fixed energy of GCR, e.g., median [*Ahluwalia et al.*, 2010] or effective [*Alanko et al.*, 2003; *Asvestari et al.*, 2017] ones. However, more accurate is to evaluate the parameters of the GCR energy spectrum, described in the form of a force-field approximation [*Gleeson and Axford*, 1968; *Caballero-Lopez and Moraal*, 2004], directly from NM count rates [*Usoskin et al.*, 2002].

To assess the GCR spectrum (more exactly, the modulation potential ϕ) from NM data, one needs to know the yield-function of the NM to energetic particles, that describes the sensitivity of a detector to primary particles as a function of their energy [*Dorman*, 2004].

The NM yield function is typically calculated using a full Monte-Carlo simulation of the nucleonic-muon-electromagnetic atmospheric cascade triggered by primary CR particles [*Clem and Dorman*, 2000; *Mishev et al.*, 2013; *Mangeard et al.*, 2016a] but is still somewhat uncertain in the low and high energy ranges. In particular, it has been shown by *Mishev et al.* [2013] that the lateral spread of atmospheric cascades enhances the NM sensitivity to high energy CR, considering the finite deadtime of the detector. Sometimes the yield function is defined empirically from the NM latitudinal surveys [e.g., *Caballero-Lopez and Moraal*, 2012] but it is limited to low energy range (below about 15 GeV) and cannot be applied to higher energy CRs whose contribution to the NM count rate is high [*Usoskin et al.*, 2005]. Moreover, a calibration to direct GCR spectral data, obtained by space- or balloon-borne measurements, is required for each individual NM to account for the exact surrounding (electronic setup, building, etc) of the NM [e.g., *Mangeard et al.*, 2016b].

First attempts to link the NM count rate with the modulation potential were made a while ago [*O'Brien and Burke*, 1973]. However, earlier studies were limited in the use of calibration to balloon-borne data measuring the GCR spectrum in the energy range below a few GeV/nuc, or to space-borne data in low-energy range of below a few hundred MeV/nuc, which does not correspond to the effective energy of NMs. A more systematic calibration was performed later [*Usoskin et al.*, 2005; *Usoskin et al.*, 2011] using the GCR spectral measurements in a wide energy range performed by the AMS-01 space experiment during a quiet period in June 1998 [*Alcaraz et al.*, 2000, 2002] and balloon-borne measurements MASS89 [*Webber et al.*, 1991] for a very active solar period in September 1989. A significant source of uncertainty of linking NM count rates to the heliospheric modulation is related to the NM yield function. Earlier yield functions [*Debrunner et al.*, 1982;

Clem and Dorman, 2000; *Matthiä*, 2009] systematically underestimated the contribution of high-energy nucleons. This led, in particular, to a clear discrepancy between modelled and experimental results of the NM latitudinal surveys [*Clem and Dorman*, 2000; *Mishev et al.*, 2013]. Accordingly, an *ad hoc* empirical correction was used by *Usoskin et al.* [2005] and *Usoskin et al.* [2011] to "match" models with observation.

A new NM yield function, computed by *Mishev et al.* [2013], explicitly accounts for the finite lateral spread of the cosmic-ray induced atmospheric cascade and the dead-time of the detector. This effects has eliminated problems with the comparison of modelled and measured NM responses, in particular for latitude surveys [*Gil et al.*, 2015]. Another recent NM yield function by [*Mangeard et al.*, 2016b] also models the NM count rate in a realistic way.

New systematic measurements of the GCR proton spectra performed by the PAMELA (Payload for Antimatter Matter Exploration and Light-nuclei Astrophysics) detector in space [*Adriani et al.*, 2011, 2014] made a more detailed comparison possible, for the period 2006–2009 [*Adriani et al.*, 2013]. A recent reconstruction of the modulation potential for the NM era was performed by *Usoskin et al.* [2017] using this PAMELA dataset and the NM yield function by *Mishev et al.* [2013]. Similar efforts were perfromed by *Corti et al.* [2016] and *Ghelfi et al.* [2016]. Taking into account different local interstellar spectra and yield-function models used there, the results are consistent with each other. The data, analyzed there, corresponded to a minimum of the solar cycle and very low modulation of GCR. Accordingly, the validity of the relation between direct spectrum measurements and models based on NM data remain unresolved for the full range of the modulation. Recently, a new dataset of PAMELA measurements of the GCR proton

spectra has been published [*Martucci et al.*, 2018] for the period 2010–2014, covering the rising and maximum phase of solar cycle 24. Thus, presently we have direct measurements of GCR proton spectra for the period 2006–2014 from the late declining phase of solar cycle 23 to the maximum of cycle 24 (see the hatched area in Figure 1), which allows one to study the relation between measured and modelled spectra in great details. This forms the subject of the present work.

2. Datasets

2.1. PAMELA data

PAMELA spectrometer [*Adriani et al.*, 2011] is a space-borne particle detector on board the *Resurs-DK1* satellite on a highly inclined (about 70°) elliptical low orbit. The instrument was in nearly continuous operation from the launch in June 2006 until January 2016. PAMELA provided measurements of charged energetic particles with energy above 80 MeV. Here we use published data (digital data are available in the ASDC database at tools.asdc.asi.it/CosmicRays/) of proton spectra measurements averaged over roughly Carrington rotation period, as summarized in Table 1. Original data for the period 2006–2009 (intervals 1–47 in the Table) were published by *Adriani et al.* [2013] and for 2010–2014 (intervals 48–83) by *Martucci et al.* [2018]. Intervals 47 and 48 overlap, bridging the first and the second sets of data, as needed for a consistency check. These measured spectra were fitted by the force-field model to estimate the modulation potential as described in Section 3.

2.2. NM data

Here we used data from long-operating sea-level (sub)polar NMs with stable parameters over the analyzed period of 2006–2014. The question of long-term stability was considered elsewhere [see Figure 5 in *Usoskin et al.*, 2017], and we selected Oulu (9NM64, geomagnetic cutoff rigidity P_c = 0.8 GV, location 25.47°E 65.05°), Inuvik (18NM64, P_c = 0.3 GV, 133.72°W 68.36°N) and Kerguelen (18NM64, P_c = 1.1 GV, 70.25°E 49.35°S) NMs. Count rates (corrected for barometric pressure and efficiency) of these NMs for the same intervals (Table 1) were collected from NMDB (nmdb.eu) and IZMIRAN (cr0.izmiran.ru/common/links.htm) databases for Inuvik and Kerguelen NMs and directly from the Oulu NM database (cosmicrays.oulu.fi).

2.3. Other balloon- and space-borne data

To compare the results of this study, we also employed other measurements of CR spectra performed onboard balloon flights or the AMS space missions (see Table 2). Exact periods and measured spectra for balloon and AMS data were taken from the ASDC database with the original references to [*Seo et al.*, 1991, 2001; *Webber et al.*, 1991; *Bellotti et al.*, 1999; *Boezio et al.*, 1999, 2003; *Alcaraz et al.*, 2000; *Menn et al.*, 2000; *Wang et al.*, 2002; *Shikaze et al.*, 2007; *Adriani et al.*, 2013; *Aguilar et al.*, 2015; *Abe et al.*, 2016].

3. Fitting of the data with model spectra

Each measured spectrum of protons (Tables 1 and 2) was fitted with the force-field model to define the corresponding modulation potential ϕ. The force-field model links the energy spectrum of GCR particles of a given type (protons, α-particles etc.) near Earth, J, with their reference intensity outside the heliosphere, called the local interstellar

spectrum (LIS) J_{LIS}:

$$J_i(T,\phi) = J_{\mathrm{LIS}_i}(T+\Phi_i)\frac{T(T+2T_r)}{(T+\Phi_i)(T+\Phi_i+2T_r)} \tag{1}$$

where T is the kinetic energy per nucleon, and $T_r = 0.938$ GeV is the proton's rest mass, $\Phi_i = \phi \cdot (eZ_i/A_i)$ is the mean energy loss of the GCR particle inside the heliosphere, Z_i and A_i are the charge and mass numbers of the nucleus of type i. The force-field approximation is obtained as an analytical solution (in the form of characteristic curves) of the heavily simplified GCR transport equation [*Gleeson and Axford*, 1968; *Caballero-Lopez and Moraal*, 2004], where all the modulation effects are reduced to a single parameter ϕ called the modulation potential. Although it has little physical sense because of the heavy simplified assumptions (spherical symmetry, steady state, adiabatic changes), the force-field model provides a very good and useful parametrization of the near-Earth GCR spectrum [e.g. *Vainio et al.*, 2009]. The exact value of the modulation parameter depends on the reference LIS [*Usoskin et al.*, 2005; *Herbst et al.*, 2010; *Asvestari et al.*, 2017]. Here we used a recent estimate of the proton LIS by *Vos and Potgieter* [2015], who provided a parametrization of LIS using recent data:

$$J_{\mathrm{LIS}} = 2.7 \cdot 10^3 \ \frac{T^{1.12}}{\beta^2}\left(\frac{T+0.67}{1.67}\right)^{-3.93}, \tag{2}$$

where $\beta = v/c$ is the ratio of the proton's velocity to the speed of light, J and T are given in units of $[\mathrm{m}^2\ \mathrm{sec\ sr\ GeV/nuc}]^{-1}$ and GeV/nucleon, respectively. This LIS is shown as the dashed curve in Fig. 2.

The measured proton spectra were fitted by the force-field model (Equations 1 and 2) using the χ^2 method. For a value of ϕ the merit function χ^2 was calculated as

$$\chi^2 = \sum_j \left(\frac{J_{\mathrm{mod}}(T_j) - J_{\mathrm{meas}}(T_j)}{\sigma_j}\right)^2, \tag{3}$$

where T_j is the mean value of the energy in the j-th bin in the spectrum, modelled and measured mean intensities in this energy bin are $J_{\rm mod}(T_j)$ and $J_{\rm meas}(T_j)$, respectively, and σ_j is the uncertainty of the measured intensity. Here we fitted the spectra in the energy range 1 – 30 GeV which includes $n = 42$ energy bins. Accordingly, the number of degrees of freedom (DoFs) is $(n - 1) = 41$. Two examples of the fit are shown in Figure 2. One example is for the interval 48 (see Table 1) with the lowest value of the modulating potential (351 MV). The other example is for the interval 77 with the highest value of ϕ (755 MV). The corresponding dependences of the merit function χ^2 on values of ϕ are shown in panels B and C. The best-fit values of the modulation potential are taken as those corresponding to the minimum value of $\chi^2_{\rm min}$ as shown by vertical arrows in the panels. The 68% confidence interval of the modulation potential is defined in a standard way as that bounded by values of ϕ corresponding to $\chi^2 = (\chi^2_{\rm min} + 1)$, as illustrated in the Figure by dotted arrows. Thus, the values of $\phi = 351 \pm 12$ MV and 755 ± 12.5 MV are defined and enter Table 1 for intervals 48 and 77, respectively.

The values of $\chi^2_{\rm min}$ appear to be 9.4 and 30.9 for the intervals 48 and 77, respectively. When normalized per degree of freedom, it yields 0.23 and 0.75 per DoF, respectively. A histogram distribution of the $\chi^2_{\rm min}$ values for all the 83 intervals is shown in Figure 3. One can see that the median of the distribution lies close to 16 (the mode ≈ 12), which corresponds to about 0.4 per DoF, and is reasonably described by a log-normal distribution (the red curve). Such low (below unity per DoF) values and the smooth distribution of $\chi^2_{\rm min}$ suggest that, while the fit is correct, the uncertainties of PAMELA data are likely overestimated, in a sense that the real spread of data-points is smaller than expected from the official error bars. On the other hand, the formal uncertainties of the spectra,

provided by PAMELA data, include two types of errors, statistical and systematic, which are comparable to each other. The latter was estimated in a conservative manner leading to quite a conservative error estimate. However, this does not undermine the way of the definition of best-fit values of ϕ and does not affect the present analysis.

Spectra for all other PAMELA intervals as well as for other data were fitted in the same way, and the best fit modulation potentials were defined along with its 68% confidence interval. The corresponding values were gathered in Tables 1 and 2.

4. Comparison with NM data

In Figure 4 we show a scatter plot of the fitted modulation potential ϕ for all PAMELA intervals and balloon flights as a function of the (inverted) count rate N of the three selected NMs for the same time intervals. Since an approximately linear relation $\phi = A/N + B$ between these variables is expected [*Usoskin et al.*, 2017; *Santiago et al.*, 2018], we plot, as X-axis, the inverted count rate per counter. One can see that both PAMELA datasets (red stars), balloon-borne data (open circles) and AMS data (filled circles) all lie along a nearly linear dependence (the best-fit linear dependence was built using only PAMELA data), which is shown by the red line. Red stars lie much more compact than other datapoints, because they were obtained by the same instrument, similarly presented and fitted, while isolated balloon-borne data lead to a large scatter.

We also depict in Figure 4 theoretically expected relations between ϕ and N. The theoretically expected NM count rate at given time t and atmospheric depth h was computed as [see, e.g. *Usoskin et al.*, 2017]

$$N(T,h) = \frac{1}{\kappa} \sum_i \int_{T_{c,i}}^{\infty} J_i(T,t) \cdot Y_i(T.h) \cdot dT, \tag{4}$$

where the summation is over different types of primary cosmic rays (protons, $\alpha-$particles, etc), J_i is the spectrum of these particles in the near-Earth space outside the atmosphere and magnetoshere, Y_i is the yield function, and κ is a scaling factor (typically in the range 0.8–1.25) correcting for the "non-ideality" (local surrounding, exact electronic setup, efficiency of counters, etc, see *Mangeard et al.* [2016a]) of each NM. Scaling factors κ were adopted from our previous work [*Usoskin et al.*, 2017] as 1.121, 1.254 and 1.078 for Oulu, Inuvik and Kerguelen NMs, respectively. NM yield functions were adopted from two recent models: [*Mishev et al.*, 2013, – called Mi13 henceforth] and [*Mangeard et al.*, 2016b, – Ma16], both built on a full Monte-Carlo simulation of the CR-induced nucleonic cascade in the atmosphere.

It is important to consider also $\alpha-$particles (effectively including heavier species because of the similar A/Z ratio) separately from protons since they are modulated differently and contribute 30–50% to the overall count rate of a NM [*Usoskin et al.*, 2011; *Caballero-Lopez and Moraal*, 2012]. For $\alpha-$particles (including the heavier species) we used the same LIS form as for protons (Eq. 2) but with the weight of 0.3 (in the number of nucleons) similarly to *Usoskin et al.* [2011].

The corresponding theoretical dependencies are shown in Figure 4 as black dashed and blue dotted lines for the models Mi13 and Ma16, respectively. Although both models predict a nearly linear relation between ϕ and $1/N$, the slopes are different for the two models and they both differ from the empirical relation, shown by the red line. The result based on Mi13 is more or less consistent with the data for weak activity with $\phi < 500$ MV. This led *Usoskin et al.* [2017] to a conclusion that the Mi13 yield function is fully consistent with the early PAMELA data covering the solar minimum 2006–2009. However,

a significant divergence can be observed at higher activity ($\phi > 600$ MV). In order to illustrate this, we show (Figure 5) time profiles of the modulation potential obtained here from the PAMELA data (dot with error bars) and that reconstructed by *Usoskin et al.* [2017] from NM data using the Mi13 yield function (red curve). One can see that, indeed, the first period of PAMELA data 2006–2009 depicts good agreement, but the NM-based reconstruction seems to underestimate the modulation potential systematically by up to 100 MV (or 10%) during higher activity periods. The results based on Ma16 yield function diverge even greater (up to 200 MV or 20%, not shown here). This pattern is persistent for all the three NMs considered here.

The results shown in Figures 4 and 5 imply that there is a discrepancy between the energy spectra of GCR protons directly measured in space and those formally reconstructed from ground-based NM data. The discrepancy is not large (being within the full range of 100 MV) but systematic. The observed relation between the modulation potential ϕ and the inverted NM count rate appears systematically weaker (the slope is steeper) than expected from the numerical models. We found that both used yield-function models disagree with the data, but the results based on Mi13 lie closer to the experimental data than those based on Ma16. Although the exact reason for the discrepancy is unknown, we may speculate on three possible sources. One possibility is related to a possible degradation of the PAMELA sensitivity with time, leading to an overestimated modulation potential during the late years. However, considering the thoroughness of the PAMELA team work and the fact that the spectral shape is not distorted, this option looks unlikely, which is consistent with independent balloon-borne data. Other, more likely possibilities are related to the modelled yield function of NM. Since the observed dependence on the

modulation potential is weaker than the modelled one (i.e., the NM count rate is less sensitive to changes of the modulation than expected from the models), it can be either an underestimate of the NM yield function at the high-energy tail or its overestimate in the low-energy range. On the other hand, reconstructions of the energy spectra of solar energetic particles from NM data [e.g., *Mishev and Usoskin*, 2016; *Kocharov et al.*, 2017] suggest that the low-energy part of the NM yield function by *Mishev et al.* [2013] is more or less correct.

At present we are not able to identify the source of the discrepancy between the modelled and measured spectra for periods of high solar activity, but can speculate that a likely reason for the discrepancy is an underestimate of the NM yield function in high energy range. More investigation is needed, which is planned for further research.

5. Conclusions

In this work we have compared GCR proton spectra directly measured by the PAMELA experiment during 83 time intervals covering the period 2006–2014 with the data of polar neutron monitors for the same time intervals. The following conclusions have been made:

1. The GCR proton spectra measured by PAMELA were parameterized by the force-field model. The parametrization works well within the range of the modulation potential values from 350 – 750 MV for the LIS by *Vos and Potgieter* [2015].

2. The obtained values of the modulation potential are in good agreement with those calculated from the data of the world neutron monitor network [*Usoskin et al.*, 2017] for the period of low solar activity 2006–2012, but diverge during the maximum of solar cycle 24 around 2013–2014.

3. The empirical relation between the modulation potential and the (inverted) NM count rate appears somewhat steeper than the modelled one. The discrepancy is not big (up to 10–20% during periods of high activity) but systematic. The results based on the NM yield function by *Mishev et al.* [2013] lie closer to the experimental points than those based on the results by *Mangeard et al.* [2016b].

4. The reason for the discrepancy is unclear. We speculate that a likely reason is a possible underestimate of the NM yield function in the high energy range. A systematic error in PAMELA data is less likely. More investigation is needed with the use of an independent dataset, e.g., GCR spectra measured by the AMS experiment [*Aguilar et al.*, 2015].

Acknowledgments. Data of NMs count rates were obtained from the NMDB (www.nmdb.eu), IZMIRAN (cr0.izmiran.ru/common/links.htm) and Oulu NM (cosmicrays.oulu.fi) databases. NMDB database, founded under the European Union's FP7 programme (contract no. 213007), is not responsible for the data quality. PIs and teams of all the ballon- and space-borne experiments as well as ground-based neutron monitors whose data were used here, are gratefully acknowledged. This work was partially supported by the ReSoLVE Centre of Excellence (Academy of Finland, project no. 272157). SAK acknowledges support from the Russian Foundation for Basic Research (grant 18-32-00062) and MEPhI Academic Excellence Project (Contract No. 02.a03.21.0005)

References

Abe, K., H. Fuke, S. Haino, T. Hams, M. Hasegawa, A. Horikoshi, A. Itazaki, K. C. Kim, T. Kumazawa, A. Kusumoto, M. H. Lee, Y. Makida, S. Matsuda, Y. Matsukawa,

K. Matsumoto, J. W. Mitchell, Z. Myers, J. Nishimura, M. Nozaki, R. Orito, J. F. Ormes, N. Picot-Clemente, K. Sakai, M. Sasaki, E. S. Seo, Y. Shikaze, R. Shinoda, R. E. Streitmatter, J. Suzuki, Y. Takasugi, K. Takeuchi, K. Tanaka, N. Thakur, T. Yamagami, A. Yamamoto, T. Yoshida, and K. Yoshimura (2016), Measurements of Cosmic-Ray Proton and Helium Spectra from the BESS-Polar Long-duration Balloon Flights over Antarctica, *Astrophys. J.*, *822*, 65, doi:10.3847/0004-637X/822/2/65.

Adriani, O., G. C. Barbarino, G. A. Bazilevskaya, R. Bellotti, M. Boezio, E. A. Bogomolov, L. Bonechi, M. Bongi, V. Bonvicini, S. Borisov, S. Bottai, A. Bruno, F. Cafagna, D. Campana, R. Carbone, P. Carlson, M. Casolino, G. Castellini, L. Consiglio, M. P. De Pascale, C. De Santis, N. De Simone, V. Di Felice, A. M. Galper, W. Gillard, L. Grishantseva, G. Jerse, A. V. Karelin, S. V. Koldashov, S. Y. Krutkov, A. N. Kvashnin, A. Leonov, V. Malakhov, V. Malvezzi, L. Marcelli, A. G. Mayorov, W. Menn, V. V. Mikhailov, E. Mocchiutti, A. Monaco, N. Mori, N. Nikonov, G. Osteria, F. Palma, P. Papini, M. Pearce, P. Picozza, C. Pizzolotto, M. Ricci, S. B. Ricciarini, L. Rossetto, R. Sarkar, M. Simon, R. Sparvoli, P. Spillantini, Y. I. Stozhkov, A. Vacchi, E. Vannuccini, G. Vasilyev, S. A. Voronov, Y. T. Yurkin, J. Wu, G. Zampa, N. Zampa, and V. G. Zverev (2011), PAMELA Measurements of Cosmic-Ray Proton and Helium Spectra, *Science*, *332*, 69–72, doi:10.1126/science.1199172.

Adriani, O., G. C. Barbarino, G. A. Bazilevskaya, R. Bellotti, M. Boezio, E. A. Bogomolov, M. Bongi, V. Bonvicini, S. Borisov, S. Bottai, A. Bruno, F. Cafagna, D. Campana, R. Carbone, P. Carlson, M. Casolino, G. Castellini, M. P. De Pascale, C. De Santis, N. De Simone, V. Di Felice, V. Formato, A. M. Galper, L. Grishantseva, A. V. Karelin, S. V. Koldashov, S. Koldobskiy, S. Y. Krutkov, A. N. Kvashnin, A. Leonov,

V. Malakhov, L. Marcelli, A. G. Mayorov, W. Menn, V. V. Mikhailov, E. Mocchiutti, A. Monaco, N. Mori, N. Nikonov, G. Osteria, F. Palma, P. Papini, M. Pearce, P. Picozza, C. Pizzolotto, M. Ricci, S. B. Ricciarini, L. Rossetto, R. Sarkar, M. Simon, R. Sparvoli, P. Spillantini, Y. I. Stozhkov, A. Vacchi, E. Vannuccini, G. Vasilyev, S. A. Voronov, Y. T. Yurkin, J. Wu, G. Zampa, N. Zampa, V. G. Zverev, M. S. Potgieter, and E. E. Vos (2013), Time Dependence of the Proton Flux Measured by PAMELA during the 2006 July-2009 December Solar Minimum, *Astrophys. J.*, *765*, 91, doi:10.1088/0004-637X/765/2/91.

Adriani, O., G. C. Barbarino, G. A. Bazilevskaya, R. Bellotti, M. Boezio, E. A. Bogomolov, M. Bongi, V. Bonvicini, S. Bottai, A. Bruno, F. Cafagna, D. Campana, R. Carbone, P. Carlson, M. Casolino, G. Castellini, M. P. De Pascale, C. De Santis, N. De Simone, V. Di Felice, V. Formato, A. M. Galper, U. Giaccari, A. V. Karelin, M. D. Kheymits, S. V. Koldashov, S. Koldobskiy, S. Y. Krut'kov, A. N. Kvashnin, A. Leonov, V. Malakhov, L. Marcelli, M. Martucci, A. G. Mayorov, W. Menn, V. V. Mikhailov, E. Mocchiutti, A. Monaco, N. Mori, R. Munini, N. Nikonov, G. Osteria, P. Papini, M. Pearce, P. Picozza, C. Pizzolotto, M. Ricci, S. B. Ricciarini, L. Rossetto, R. Sarkar, M. Simon, R. Sparvoli, P. Spillantini, Y. I. Stozhkov, A. Vacchi, E. Vannuccini, G. I. Vasilyev, S. A. Voronov, J. Wu, Y. T. Yurkin, G. Zampa, N. Zampa, and V. G. Zverev (2014), The PAMELA Mission: Heralding a new era in precision cosmic ray physics, *Phys. Rep.*, *544*, 323–370, doi:10.1016/j.physrep.2014.06.003.

Aguilar, M., D. Aisa, B. Alpat, A. Alvino, G. Ambrosi, K. Andeen, L. Arruda, N. Attig, P. Azzarello, A. Bachlechner, and et al. (2015), Precision Measurement of the Proton Flux in Primary Cosmic Rays from Rigidity 1 GV to 1.8 TV with the Alpha Magnetic

Spectrometer on the International Space Station, *Physical Review Letters*, *114*(17), 171103, doi:10.1103/PhysRevLett.114.171103.

Ahluwalia, H. S., M. M. Fikani, and R. C. Ygbuhay (2010), Rigidity dependence of 11 year cosmic ray modulation: Implication for theories, *J. Geophys. Res.*, *115*, A07101, doi:10.1029/2009JA014798.

Alanko, K., I. G. Usoskin, K. Mursula, and G. A. Kovaltsov (2003), Heliospheric modulation strength: Effective neutron monitor energy, *Adv. Space Res.*, *32*, 615–620, doi:10.1016/S0273-1177(03)00348-X.

Alcaraz, J., B. Alpat, G. Ambrosi, H. Anderhub, L. Ao, A. Arefiev, P. Azzarello, E. Babucci, L. Baldini, M. Basile, D. Barancourt, F. Barao, G. Barbier, G. Barreira, R. Battiston, R. Becker, U. Becker, L. Bellagamba, P. Béné, J. Berdugo, P. Berges, B. Bertucci, A. Biland, S. Bizzaglia, S. Blasko, G. Boella, M. Boschini, M. Bourquin, L. Brocco, G. Bruni, M. Buenerd, J. D. Burger, W. J. Burger, X. D. Cai, C. Camps, P. Cannarsa, M. Capell, D. Casadei, J. Casaus, G. Castellini, C. Cecchi, Y. H. Chang, H. F. Chen, H. S. Chen, Z. G. Chen, N. A. Chernoplekov, T. H. Chiueh, Y. L. Chuang, F. Cindolo, V. Commichau, A. Contin, P. Crespo, M. Cristinziani, J. P. da Cunha, T. S. Dai, J. D. Deus, N. Dinu, L. Djambazov, I. D'Antone, Z. R. Dong, P. Emonet, J. Engelberg, F. J. Eppling, T. Eronen, G. Esposito, P. Extermann, J. Favier, E. Fiandrini, P. H. Fisher, G. Fluegge, N. Fouque, Y. Galaktionov, M. Gervasi, P. Giusti, D. Grandi, O. Grimm, W. Q. Gu, K. Hangarter, A. Hasan, V. Hermel, H. Hofer, M. A. Huang, W. Hungerford, M. Ionica, R. Ionica, M. Jongmanns, K. Karlamaa, W. Karpinski, G. Kenney, J. Kenny, W. Kim, A. Klimentov, R. Kossakowski, V. Koutsenko, M. Kraeber, G. Laborie, T. Laitinen, G. Lamanna, G. Laurenti, A. Lebedev, S. C. Lee,

G. Levi, P. Levtchenko, C. L. Liu, H. T. Liu, I. Lopes, G. Lu, Y. S. Lu, K. Lübelsmeyer, D. Luckey, W. Lustermann, C. Maña, A. Margotti, F. Mayet, R. R. McNeil, B. Meillon, M. Menichelli, A. Mihul, A. Mourao, A. Mujunen, F. Palmonari, A. Papi, I. H. Park, M. Pauluzzi, F. Pauss, E. Perrin, A. Pesci, A. Pevsner, M. Pimenta, V. Plyaskin, V. Pojidaev, M. Pohl, V. Postolache, N. Produit, P. G. Rancoita, D. Rapin, F. Raupach, D. Ren, Z. Ren, M. Ribordy, J. P. Richeux, E. Riihonen, J. Ritakari, U. Roeser, C. Roissin, R. Sagdeev, G. Sartorelli, A. Schultz von Dratzig, G. Schwering, G. Scolieri, E. S. Seo, V. Shoutko, E. Shoumilov, R. Siedling, D. Son, T. Song, M. Steuer, G. S. Sun, H. Suter, X. W. Tang, S. C. C. Ting, S. M. Ting, M. Tornikoski, J. Torsti, J. Trümper, J. Ulbricht, S. Urpo, I. Usoskin, E. Valtonen, J. Vandenhirtz, F. Velcea, E. Velikhov, B. Verlaat, I. Vetlitsky, F. Vezzu, J. P. Vialle, G. Viertel, D. Vité, H. Von Gunten, S. Waldmeier Wicki, W. Wallraff, B. C. Wang, J. Z. Wang, Y. H. Wang, K. Wiik, C. Williams, S. X. Wu, P. C. Xia, J. L. Yan, L. G. Yan, C. G. Yang, M. Yang, S. W. Ye, P. Yeh, Z. Z. Xu, H. Y. Zhang, Z. P. Zhang, D. X. Zhao, G. Y. Zhu, W. Z. Zhu, H. L. Zhuang, A. Zichichi, and B. Zimmermann (2000), Cosmic protons, *Phys. Lett. B*, *490*, 27–35, doi:10.1016/S0370-2693(00)00970-9.

Alcaraz, J., B. Alpat, G. Ambrosi, H. Anderhub, L. Ao, A. Arefiev, P. Azzarello, E. Babucci, L. Baldini, M. Basile, D. Barancourt, F. Barao, G. Barbier, G. Barreira, R. Battiston, R. Becker, U. Becker, L. Bellagamba, P. Bene, J. Berdugo, P. Berges, B. Bertucci, A. Biland, S. Bizzaglia, S. Blasko, G. Boella, M. Boschini, M. Bourquin, L. Brocco, G. Bruni, M. Buenerd, J. D. Burger, W. J. Burger, X. D. Cai, C. Camps, P. Cannarsa, M. Capell, D. Casadei, J. Casaus, G. Castellini, C. Cecchi, Y. H. Chang, H. F. Chen, H. S. Chen, Z. G. Chen, N. A. Chernoplekov, T. H. Chiueh, Y. L. Chuang,

F. Cindolo, V. Commichau, A. Contin, P. Crespo, M. Cristinziani, J. P. da Cunha, T. S. Dai, J. D. Deus, N. Dinu, L. Djambazov, I. DAntone, Z. R. Dong, P. Emonet, J. Engelberg, F. J. Eppling, T. Eronen, G. Esposito, P. Extermann, J. Favier, E. Fiandrini, P. H. Fisher, G. Fluegge, N. Fouque, Y. Galaktionov, M. Gervasi, P. Giusti, D. Grandi, O. Grimm, W. Q. Gu, K. Hangarter, A. Hasan, V. Hermel, H. Hofer, M. A. Huang, W. Hungerford, M. Ionica, R. Ionica, M. Jongmanns, K. Karlamaa, W. Karpinski, G. Kenney, J. Kenny, W. Kim, A. Klimentov, R. Kossakowski, V. Koutsenko, M. Kraeber, G. Laborie, T. Laitinen, G. Lamanna, G. Laurenti, A. Lebedev, S. C. Lee, G. Levi, P. Levtchenko, C. L. Liu, H. T. Liu, I. Lopes, G. Lu, Y. S. Lu, K. Lübelsmeyer, D. Luckey, W. Lustermann, C. Man˜a, A. Margotti, F. Mayet, R. R. McNeil, B. Meillon, M. Menichelli, A. Mihul, A. Mourao, A. Mujunen, F. Palmonari, A. Papi, I. H. Park, M. Pauluzzi, F. Pauss, E. Perrin, A. Pesci, A. Pevsner, M. Pimenta, V. Plyaskin, V. Pojidaev, V. Postolache, N. Produit, P. G. Rancoita, D. Rapin, F. Raupach, D. Ren, Z. Ren, M. Ribordy, J. P. Richeux, E. Riihonen, J. Ritakari, U. Roeser, C. Roissin, R. Sagdeev, G. Sartorelli, A. Schultz von Dratzig, G. Schwering, G. Scolieri, E. S. Seo, V. Shoutko, E. Shoumilov, R. Siedling, D. Son, T. Song, M. Steuer, G. S. Sun, H. Suter, X. W. Tang, S. C. C. Ting, S. M. Ting, M. Tornikoski, J. Torsti, J. Tr umper, J. Ulbricht, S. Urpo, I. Usoskin, E. Valtonen, J. Vandenhirtz, F. Velcea, E. Velikhov, B. Verlaat, I. Vetlitsky, F. Vezzu, J. P. Vialle, G. Viertel, D. Vite, H. V. Gunten, S. W. Wicki, W. Wallraff, B. C. Wang, J. Z. Wang, Y. H. Wang, K. Wiik, C. Williams, S. X. Wu, P. C. Xia, J. L. Yan, L. G. Yan, C. G. Yang, M. Yang, S. W. Ye, P. Yeh, Z. Z. Xu, H. Y. Zhang, Z. P. Zhang, D. X. Zhao, G. Y. Zhu, W. Z. Zhu, H. L. Zhuang, A. Zichichi, and B. Zimmermann (2002), The Alpha Magnetic Spectrometer (AMS), *Nucl. Instr.*

Methods Phys. Res. A, *478*, 119–122, doi:10.1016/S0168-9002(01)01727-2.

Asvestari, E., A. Gil, G. A. Kovaltsov, and I. G. Usoskin (2017), Neutron Monitors and Cosmogenic Isotopes as Cosmic Ray Energy-Integration Detectors: Effective Yield Functions, Effective Energy, and Its Dependence on the Local Interstellar Spectrum, *J. Geophys. Res. (Space Phys.)*, *122*, 9790–9802, doi:10.1002/2017JA024469.

Bazilevskaya, G. A., E. W. Cliver, G. A. Kovaltsov, A. G. Ling, M. A. Shea, D. F. Smart, and I. G. Usoskin (2014), Solar Cycle in the Heliosphere and Cosmic Rays, *Space Sci. Rev.*, *186*, 409–435, doi:10.1007/s11214-014-0084-0.

Bellotti, R., F. Cafagna, M. Circella, C. N. de Marzo, R. L. Golden, S. J. Stochaj, M. P. de Pascale, A. Morselli, P. Picozza, S. A. Stephens, M. Hof, W. Menn, M. Simon, J. W. Mitchell, J. F. Ormes, R. E. Streitmatter, N. Finetti, C. Grimani, P. Papini, S. Piccardi, P. Spillantini, G. Basini, and M. Ricci (1999), Balloon measurements of cosmic ray muon spectra in the atmosphere along with those of primary protons and helium nuclei over midlatitude, *Phys. Rev. D*, *60*(5), 052002, doi:10.1103/PhysRevD.60.052002.

Belov, A. (2000), Large Scale Modulation: View From the Earth, *Space Sci. Rev.*, *93*, 79–105, doi:10.1023/A:1026584109817.

Boezio, M., P. Carlson, T. Francke, N. Weber, M. Suffert, M. Hof, W. Menn, M. Simon, S. A. Stephens, R. Bellotti, F. Cafagna, M. Castellano, M. Circella, C. De Marzo, N. Finetti, P. Papini, S. Piccardi, P. Spillantini, M. Ricci, M. Casolino, M. P. De Pascale, A. Morselli, P. Picozza, R. Sparvoli, G. Barbiellini, U. Bravar, P. Schiavon, A. Vacchi, N. Zampa, J. W. Mitchell, J. F. Ormes, R. E. Streitmatter, R. L. Golden, and S. J. Stochaj (1999), The Cosmic-Ray Proton and Helium Spectra between 0.4 and 200 GV, *Astrophys. J.*, *518*, 457–472, doi:10.1086/307251.

Boezio, M., V. Bonvicini, P. Schiavon, A. Vacchi, N. Zampa, D. Bergström, P. Carlson, T. Francke, P. Hansen, E. Mocchiutti, M. Suffert, M. Hof, J. Kremer, W. Menn, M. Simon, M. Ambriola, R. Bellotti, F. Cafagna, F. Ciacio, M. Circella, C. N. De Marzo, N. Finetti, P. Papini, S. Piccardi, P. Spillantini, E. Vannuccini, S. Bartalucci, M. Ricci, M. Casolino, M. P. De Pascale, A. Morselli, P. Picozza, R. Sparvoli, J. W. Mitchell, J. F. Ormes, S. A. Stephens, R. E. Streitmatter, U. Bravar, and S. J. Stochaj (2003), The cosmic-ray proton and helium spectra measured with the CAPRICE98 balloon experiment, *Astropart. Phys.*, *19*, 583–604, doi:10.1016/S0927-6505(02)00267-0.

Caballero-Lopez, R., and H. Moraal (2004), Limitations of the force field equation to describe cosmic ray modulation, *J. Geophys. Res.*, *109*, A01,101, doi:10.1029/2003JA010098.

Caballero-Lopez, R., and H. Moraal (2012), Cosmic-ray yield and response functions in the atmosphere, *J. Geophys. Res.*, *117*, A12,103, doi:10.1029/2012JA017794.

Clem, J., and L. Dorman (2000), Neutron monitor response functions, *Space Sci. Rev.*, *93*, 335–359, doi:10.1023/A:1026508915269.

Corti, C., V. Bindi, C. Consolandi, and K. Whitman (2016), Solar Modulation of the Local Interstellar Spectrum with Voyager 1, AMS-02, PAMELA, and BESS, *Astrophys. J.*, *829*, 8, doi:10.3847/0004-637X/829/1/8.

Debrunner, H., E. Flückiger, and J. Lockwood (1982), Specific yield function S(P) for a neutron monitor at sea level, in *8th Europ. Cosmic ray Symp.*, Rome, Italy.

Dorman, L. (2004), *Cosmic Rays in the Earth's Atmosphere and Underground*, Kluwer Academic Publishers, Dordrecht.

Ghelfi, A., F. Barao, L. Derome, and D. Maurin (2016), Non-parametric determination of H and He interstellar fluxes from cosmic-ray data, *Astron. Astrophys.*, *591*, A94, doi:10.1051/0004-6361/201527852.

Gil, A., I. G. Usoskin, G. A. Kovaltsov, A. L. Mishev, C. Corti, and V. Bindi (2015), Can we properly model the neutron monitor count rate?, *J. Geophys. Res.*, *120*, 7172–7178, doi:10.1002/2015JA021654.

Gleeson, L., and W. Axford (1968), Solar modulation of galactic cosmic rays, *Astrophys. J.*, *154*, 1011–1026, doi:10.1086/149822.

Herbst, K., A. Kopp, B. Heber, F. Steinhilber, H. Fichtner, K. Scherer, and D. Matthiä (2010), On the importance of the local interstellar spectrum for the solar modulation parameter, *J. Geophys. Res.*, *115*, D00I20, doi:10.1029/2009JD012557.

Kocharov, L., S. Pohjolainen, A. Mishev, M. J. Reiner, J. Lee, T. Laitinen, L. V. Didkovsky, V. J. Pizzo, R. Kim, A. Klassen, M. Karlicky, K.-S. Cho, D. E. Gary, I. Usoskin, E. Valtonen, and R. Vainio (2017), Investigating the Origins of Two Extreme Solar Particle Events: Proton Source Profile and Associated Electromagnetic Emissions, *Astrophys. J.*, *839*, 79, doi:10.3847/1538-4357/aa6a13.

Mangeard, P.-S., D. Ruffolo, A. Sáiz, S. Madlee, and T. Nutaro (2016a), Monte Carlo simulation of the neutron monitor yield function, *J. Geophys. Res.*, *121*, 7435–7448, doi:10.1002/2016JA022638.

Mangeard, P.-S., D. Ruffolo, A. Sáiz, W. Nuntiyakul, J. W. Bieber, J. Clem, P. Evenson, R. Pyle, M. L. Duldig, and J. E. Humble (2016b), Dependence of the neutron monitor count rate and time delay distribution on the rigidity spectrum of primary cosmic rays, *J. Geophys. Res. (Space Phys.)*, *121*, 11,620, doi:10.1002/2016JA023515.

Martucci, M., R. Munini, M. Boezio, V. Di Felice, O. Adriani, G. C. Barbarino, G. A. Bazilevskaya, R. Bellotti, M. Bongi, V. Bonvicini, S. Bottai, A. Bruno, F. Cafagna, D. Campana, P. Carlson, M. Casolino, G. Castellini, C. De Santis, A. M. Galper, A. V. Karelin, S. V. Koldashov, S. Koldobskiy, S. Y. Krutkov, A. N. Kvashnin, A. Leonov, V. Malakhov, L. Marcelli, N. Marcelli, A. G. Mayorov, W. Menn, M. Mergè, V. V. Mikhailov, E. Mocchiutti, A. Monaco, N. Mori, G. Osteria, B. Panico, P. Papini, M. Pearce, P. Picozza, M. Ricci, S. B. Ricciarini, M. Simon, R. Sparvoli, P. Spillantini, Y. I. Stozhkov, A. Vacchi, E. Vannuccini, G. Vasilyev, S. A. Voronov, Y. T. Yurkin, G. Zampa, N. Zampa, M. S. Potgieter, and J. L. Raath (2018), Proton Fluxes Measured by the PAMELA Experiment from the Minimum to the Maximum Solar Activity for Solar Cycle 24, *Astrophys. J. Lett.*, *854*, L2, doi:10.3847/2041-8213/aaa9b2.

Matthiä, D. (2009), The Radiation Environment in the Lower Atmosphere: A Numerical Approach, Ph.D. thesis, Christian-Albrechts-Universität zu Kiel.

Menn, W., M. Hof, O. Reimer, M. Simon, A. J. Davis, A. W. Labrador, R. A. Mewaldt, S. M. Schindler, L. M. Barbier, E. R. Christian, K. E. Krombel, J. F. Krizmanic, J. W. Mitchell, J. F. Ormes, R. E. Streitmatter, R. L. Golden, S. J. Stochaj, W. R. Webber, and I. L. Rasmussen (2000), The Absolute Flux of Protons and Helium at the Top of the Atmosphere Using IMAX, *Astrophys. J.*, *533*, 281–297, doi:10.1086/308645.

Mishev, A., and I. Usoskin (2016), Analysis of the Ground-Level Enhancements on 14 July 2000 and 13 December 2006 Using Neutron Monitor Data, *Solar Phys.*, *291*, 1225–1239, doi:10.1007/s11207-016-0877-2.

Mishev, A. L., I. G. Usoskin, and G. A. Kovaltsov (2013), Neutron monitor yield function: New improved computations, *J. Geophys. Res.*, *118*, 2783–2788, doi:10.1002/jgra.50325.

O'Brien, K., and G. Burke (1973), Calculated cosmic ray neutron monitor response to solar modulation of galactic cosmic rays, *J. Geophys. Res.*, *78*, 3013–3019.

Santiago, A., A. Lara, O. Enríquez-Rivera, and R. A. Caballero-Lopez (2018), New method to calculate the time variation of the force-field parameter, *J. Geophys. Res.: Space Phys.*, *123*, doi:10.1002/2017JA024914, 2017JA024914.

Seo, E. S., J. F. Ormes, R. E. Streitmatter, S. J. Stochaj, W. V. Jones, S. A. Stephens, and T. Bowen (1991), Measurement of cosmic-ray proton and helium spectra during the 1987 solar minimum, *Astrophys. J.*, *378*, 763–772, doi:10.1086/170477.

Seo, E. S., J. Z. Wang, H. Matsunaga, K. Anraku, M. Imori, Y. Makida, H. Matsumoto, F. B. McDonald, J. Mitchell, A. Moiseev, M. Motoki, J. Nishimura, M. Nozaki, S. Orito, J. F. Ormes, M. Otoba, T. Saeki, T. Sanuki, R. E. Streitmatter, J. Suzuki, K. Tanaka, I. Ueda, N. Yajima, T. Yamagami, A. Yamamoto, T. Yoshida, and K. Yoshimura (2001), Spectra of H and He measured in a series of annual flights, *Adv. Space Res.*, *26*, 1831–1834, doi:10.1016/S0273-1177(99)01232-6.

Shea, M. A., and D. F. Smart (2000), Fifty Years of Cosmic Radiation Data, *Space Sci. Rev.*, *93*, 229–262, doi:10.1023/A:1026500713452.

Shikaze, Y., S. Haino, K. Abe, H. Fuke, T. Hams, K. C. Kim, Y. Makida, S. Matsuda, J. W. Mitchell, A. A. Moiseev, J. Nishimura, M. Nozaki, S. Orito, J. F. Ormes, T. Sanuki, M. Sasaki, E. S. Seo, R. E. Streitmatter, J. Suzuki, K. Tanaka, T. Yamagami, A. Yamamoto, T. Yoshida, and K. Yoshimura (2007), Measurements of 0.2-20 GeV/n cosmic-ray proton and helium spectra from 1997 through 2002 with the BESS spectrometer, *Astropart. Phys.*, *28*, 154–167, doi:10.1016/j.astropartphys.2007.05.001.

Simpson, J. A. (2000), The Cosmic Ray Nucleonic Component: The Invention and Scientific Uses of the Neutron Monitor - (Keynote Lecture), *Space Sci. Rev.*, *93*, 11–32, doi:10.1023/A:1026567706183.

Usoskin, I. G., K. Alanko, K. Mursula, and G. A. Kovaltsov (2002), Heliospheric modulation strength during the neutron monitor era, *Solar Phys.*, *207*, 389–399.

Usoskin, I. G., K. Alanko-Huotari, G. A. Kovaltsov, and K. Mursula (2005), Heliospheric modulation of cosmic rays: Monthly reconstruction for 1951–2004, *J. Geophys. Res.*, *110*, A12108, doi:10.1029/2005JA011250.

Usoskin, I. G., G. A. Bazilevskaya, and G. A. Kovaltsov (2011), Solar modulation parameter for cosmic rays since 1936 reconstructed from ground-based neutron monitors and ionization chambers, *J. Geophys. Res.*, *116*, A02104, doi:10.1029/2010JA016105.

Usoskin, I. G., A. Gil, G. A. Kovaltsov, A. L. Mishev, and V. V. Mikhailov (2017), Heliospheric modulation of cosmic rays during the neutron monitor era: Calibration using PAMELA data for 2006-2010, *J. Geophys. Res. (Space Phys.)*, *122*, 3875–3887, doi:10.1002/2016JA023819.

Vainio, R., L. Desorgher, D. Heynderickx, M. Storini, E. Flückiger, R. B. Horne, G. A. Kovaltsov, K. Kudela, M. Laurenza, S. McKenna-Lawlor, H. Rothkaehl, and I. G. Usoskin (2009), Dynamics of the Earth's particle radiation environment, *Space Sci. Rev.*, *147*, 187–231, doi:10.1007/s11214-009-9496-7.

Vos, E. E., and M. S. Potgieter (2015), New Modeling of Galactic Proton Modulation during the Minimum of Solar Cycle 23/24, *Astrophys. J.*, *815*, 119, doi:10.1088/0004-637X/815/2/119.

Wang, J. Z., E. S. Seo, K. Anraku, M. Fujikawa, M. Imori, T. Maeno, N. Matsui, H. Matsunaga, M. Motoki, S. Orito, T. Saeki, T. Sanuki, I. Ueda, K. Yoshimura, Y. Makida, J. Suzuki, K. Tanaka, A. Yamamoto, T. Yoshida, T. Mitsui, H. Matsumoto, M. Nozaki, M. Sasaki, J. Mitchell, A. Moiseev, J. Ormes, R. Streitmatter, J. Nishimura, Y. Yajima, and T. Yamagami (2002), Measurement of Cosmic-Ray Hydrogen and Helium and Their Isotopic Composition with the BESS Experiment, *Astrophys. J.*, *564*, 244–259, doi:10.1086/324140.

Webber, W. R., R. L. Golden, S. J. Stochaj, J. F. Ormes, and R. E. Strittmatter (1991), A measurement of the cosmic-ray H-2 and He-3 spectra and H-2/He-4 and He-3/He-4 ratios in 1989, *Astrophys. J.*, *380*, 230–234, doi:10.1086/170578.

Table 1. Solar modulation potential ϕ values (for the LIS by *Vos and Potgieter* [2015]) fitted for the complete PAMELA dataset 2006–2014 (Section 3). Columns are: Number #, start and end of the time intervals as well as the best-fit value of ϕ with its 68% confidence interval.

#	Start	End	ϕ (MV)	#	Start	End	ϕ (MV)
1	2006-07-07	2006-07-26	561±13.5	43	2009-09-15	2009-10-11	369±17
2	2006-07-27	2006-08-22	547±13	44	2009-10-12	2009-11-07	387±17.5
3	2006-08-24	2006-09-19	536±13	45	2009-11-08	2009-12-05	363±17.5
4	2006-09-20	2006-10-16	521±13	46	2009-12-06	2010-01-01	372±17.5
5	2006-10-17	2006-11-12	522±13	47	2010-01-02	2010-01-23	371±12.5
6	2006-11-13	2006-12-04	518±12.5	48	2010-01-03	2010-01-30	351±12
7	2007-01-11	2007-02-02	508±12.5	49	2010-01-30	2010-02-27	392±11
8	2007-02-03	2007-03-02	503±13	50	2010-02-27	2010-03-26	395±10
9	2007-03-03	2007-03-29	498±13	51	2010-10-30	2010-11-26	438±10.5
10	2007-03-30	2007-04-25	481±12.5	52	2010-11-26	2010-12-24	447±10.5
11	2007-04-26	2007-05-22	474±12.5	53	2010-12-24	2011-01-20	426±10.5
12	2007-05-23	2007-06-17	475±12.5	54	2011-01-20	2011-02-16	431±10.5
13	2007-06-27	2007-07-16	467±12.5	55	2011-02-16	2011-03-16	461±11
14	2007-07-17	2007-08-12	463±13	56	2011-03-16	2011-04-12	506±11
15	2007-08-13	2007-09-06	472±13	57	2011-04-12	2011-05-09	514±10.5
16	2007-09-09	2007-10-06	461±12.5	58	2011-05-09	2011-06-05	531±12
17	2007-10-07	2007-11-02	455±13	59	2011-06-05	2011-07-03	567±11.5
18	2007-11-03	2007-11-29	446±13	60	2011-07-03	2011-07-30	526±11
19	2007-11-30	2007-12-27	444±12.5	61	2011-08-26	2011-09-22	547±11.5
20	2007-12-28	2008-01-23	453±12.5	62	2011-10-19	2011-11-16	538±11
21	2008-01-24	2008-02-19	456±12.5	63	2011-11-16	2011-12-13	525±11
22	2008-02-20	2008-03-17	454±12.5	64	2011-12-13	2012-01-09	502±11
23	2008-03-19	2008-04-14	474±13	65	2012-01-09	2012-02-06	514±11.5
24	2008-04-15	2008-05-11	463±12.5	66	2012-02-06	2012-03-04	538±11
25	2008-05-12	2008-06-07	470±12.5	67	2012-03-31	2012-04-28	594±12
26	2008-06-08	2008-07-04	468±13	68	2012-05-25	2012-06-21	588±11.5
27	2008-07-05	2008-08-01	464±13	69	2012-08-15	2012-09-11	677±11.5
28	2008-08-02	2008-08-28	452±13	70	2012-09-11	2012-10-08	641±11.5
29	2008-08-29	2008-09-11	441±12.5	71	2012-10-08	2012-11-04	686±11.5
30	2008-10-01	2008-10-21	445±13	72	2012-11-04	2012-12-02	667±11.5
31	2008-10-22	2008-11-18	417±12.5	73	2012-12-02	2012-12-29	636±11
32	2008-11-19	2008-12-15	423±12.5	74	2012-12-29	2013-01-25	619±11.5
33	2008-12-20	2009-01-11	440±12.5	75	2013-01-25	2013-02-22	602±11
34	2009-01-12	2009-02-08	414±12.5	76	2013-02-22	2013-03-21	594±11.5
35	2009-02-21	2009-03-07	396±12	77	2013-06-11	2013-07-08	755±12.5
36	2009-03-08	2009-04-03	381±12.5	78	2013-07-08	2013-08-04	714±11.5
37	2009-04-04	2009-05-01	378±12	79	2013-08-04	2013-08-31	732±12
38	2009-05-02	2009-05-28	384±12.5	80	2013-08-31	2013-09-28	741±12
39	2009-05-29	2009-06-24	389±12.5	81	2013-09-28	2013-10-25	725±12
40	2009-06-25	2009-07-21	379±12	82	2013-11-21	2013-12-19	731±12
41	2009-07-22	2009-08-18	367±12.5	83	2014-01-15	2014-02-11	735±11.5
42	2009-08-19	2009-09-14	380±12.5				

Table 2. Best-fitted values of the modulation potential ϕ (LIS as for *Vos and Potgieter* [2015]) for GCR spectra measured in various balloon- and space-borne (denoted with †) experiments.

Experiment	Start	End	ϕ (MV)
LEAP1987	1987-08-21	1987-08-21	454±29
MASS89	1989-09-05	1989-09-05	1149±23
MASS91	1991-09-23	1991-09-23	1035±50
IMAX92	1992-07-16	1992-07-17	812±30
BESS1993	1993-07-01	1993-07-01	609±30
BESS1994	1994-07-01	1994-07-01	623±32
CAPRICE1994	1994-08-08	1994-08-09	565±25
BESS1995	1995-07-25	1995-07-25	489±27
BESS1997	1997-07-27	1997-07-27	435±19
CAPRICE1998	1998-05-28	1998-05-29	619±40
BESS1998	1998-07-29	1998-07-29	519±20
BESS1999	1999-08-11	1999-08-12	606±20
BESS2000	2000-08-10	2000-08-11	1202±23
BESS-TeV	2002-08-07	2002-08-07	992±22
BESS-POLAR I	2004-12-13	2004-12-21	705±13
BESS-POLAR II	2007-12-22	2008-01-19	495±12
AMS1†	1998-06-02	1998-06-12	501±20
AMS2†	2011-05-19	2013-11-26	650±20

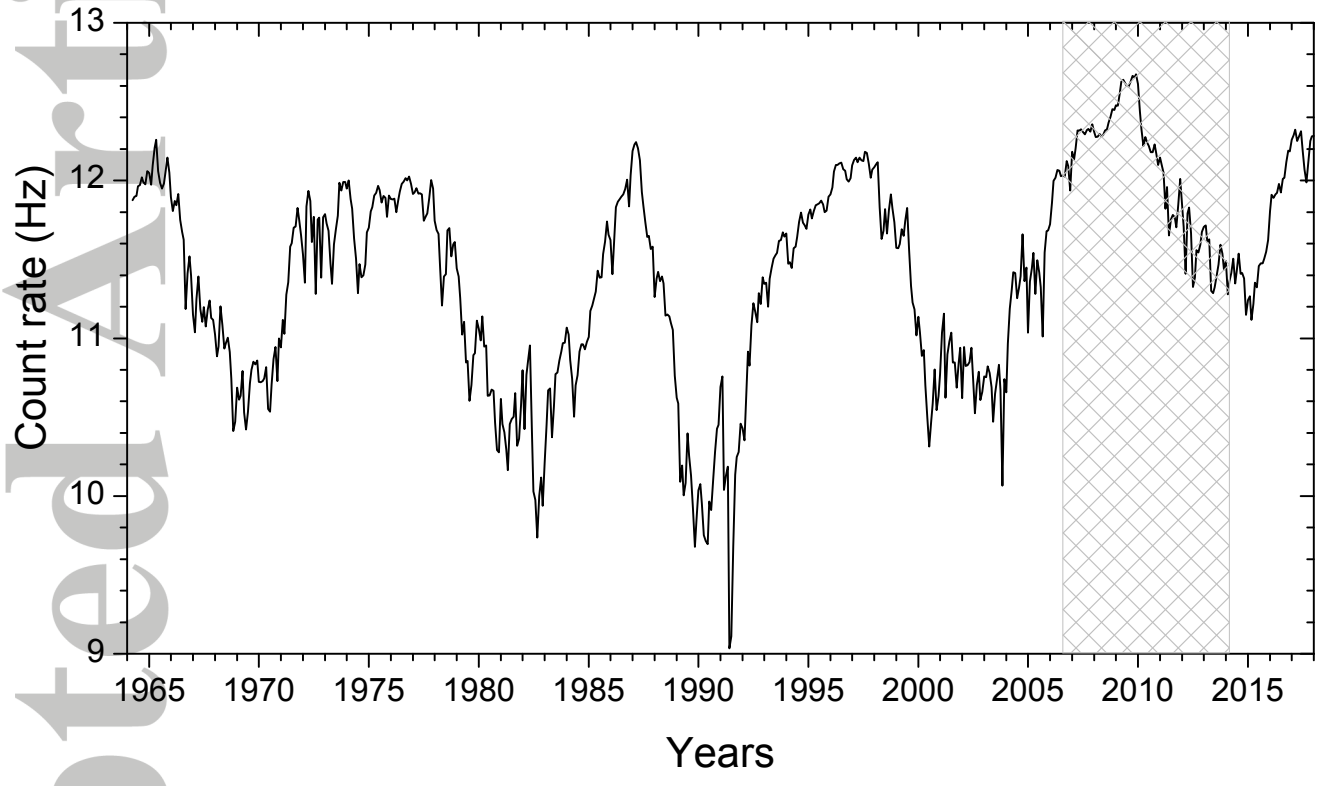

Figure 1. Monthly averaged count rate (Hz/counter) of Oulu NM (http://cosmicrays.oulu.fi) since 1964. The hatched interval depicts the period covered by PAMELA measurements (Table 1).

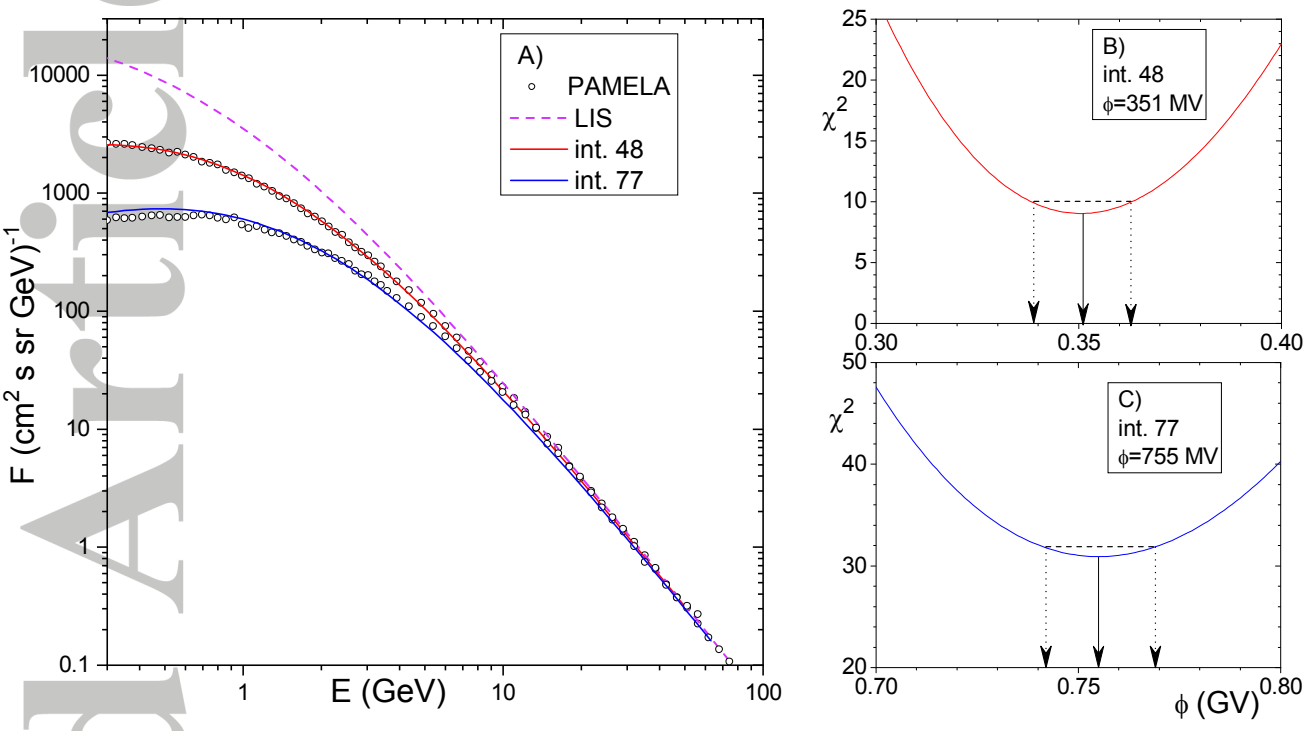

Figure 2. Examples of the fitting of a force-field model to the PAMELA proton spectrum for periods 48 (03/01/2010 – 30/01/2010) and 77 (11/06/2013 – 08/07/2013), see Table 1). Panel A: The best-fit spectra are shown as the red and blue curves, respectively. The dots represent the corresponding PAMELA data points. The purple dashed curve represents the proton LIS [*Vos and Potgieter*, 2015]. Panel B: The χ^2 statistics of the force-field model fitting to the PAMELA data for the interval 48 as shown in panel A. The best-fit value of $\phi = 351$ MV, corresponding to the minimum $\chi^2_{\rm min}$, and the 68% confidence interval, corresponding to $\chi^2_{\rm min} + 1$, shown by the solid and dashed arrows, respectively. Panel C: similar to panel B but for interval 77 (the best-fit value $\phi = 755$ MV).

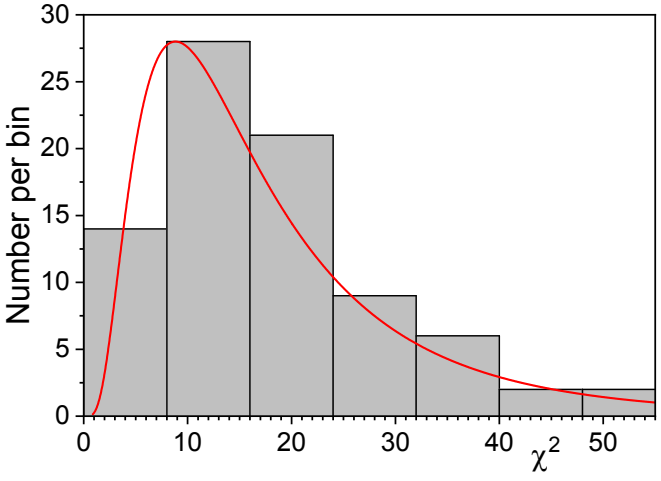

Figure 3. Distribution of the $\chi^2_{\rm min}$ values of the PAMELA spectrum fitting for the 83 intervals listed in Table 1. The best-fit log-normal distribution is shown in red.

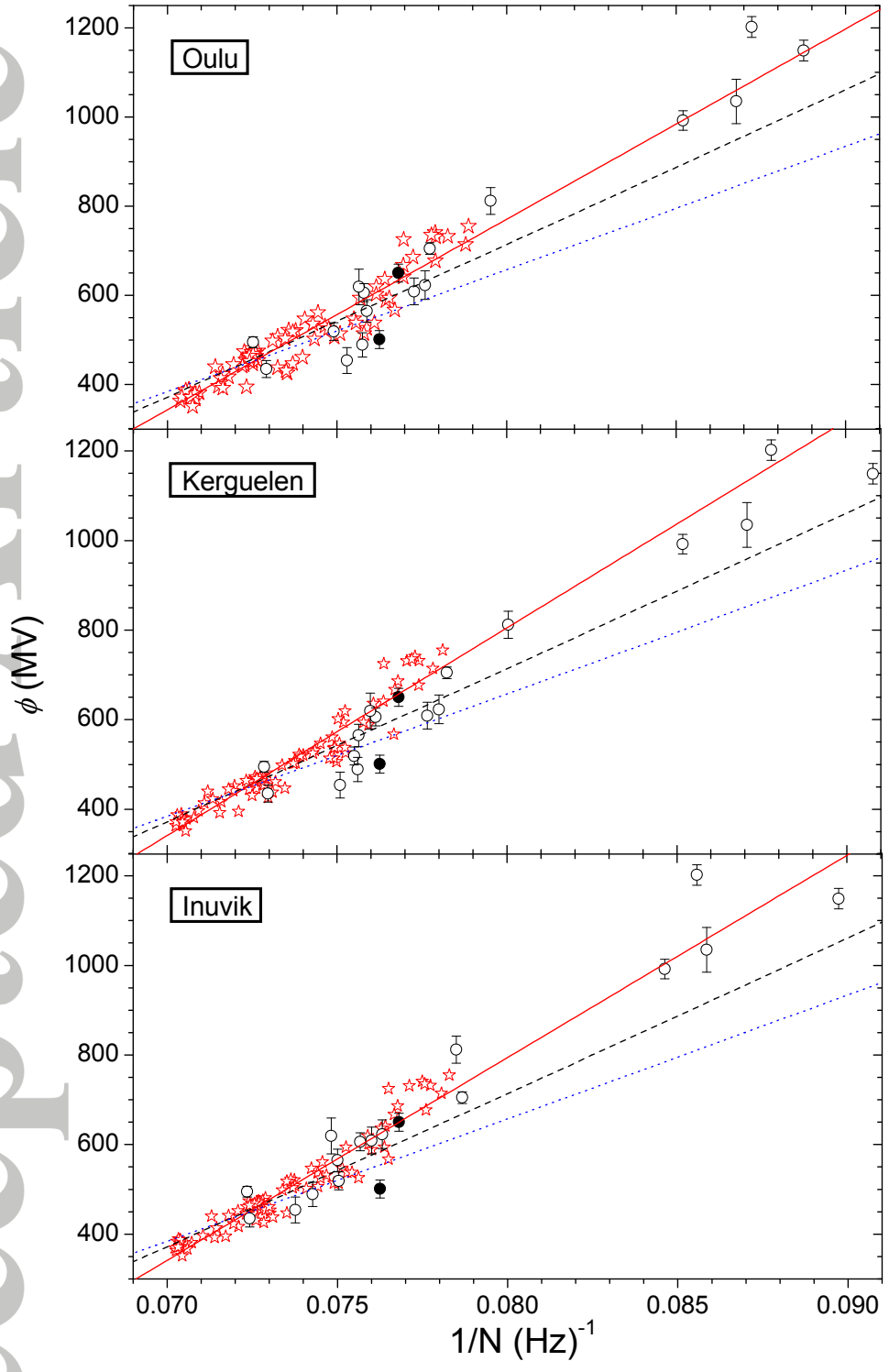

Figure 4. Relation between the modulation potential ϕ and inverted, per counter, count rate ($1/N$) of neutron monitors analyzed here: Oulu, Kerguelen and Inuvik. Red stars represent the PAMELA data periods (see Table 1), open and black dots – various balloon- and space-borne CR measurements, as listed in Table 2, respectively. The red solid line is the best-fit linear regression only for the PAMELA-based datapoints (red stars, black dots were not used for fitting), while black dashed Mi13 and blue dotted Ma16 lines depict theoretical models based on the NM yield functions by *Mishev et al.* [2013] and *Mangeard et al.* [2016a], respectively.

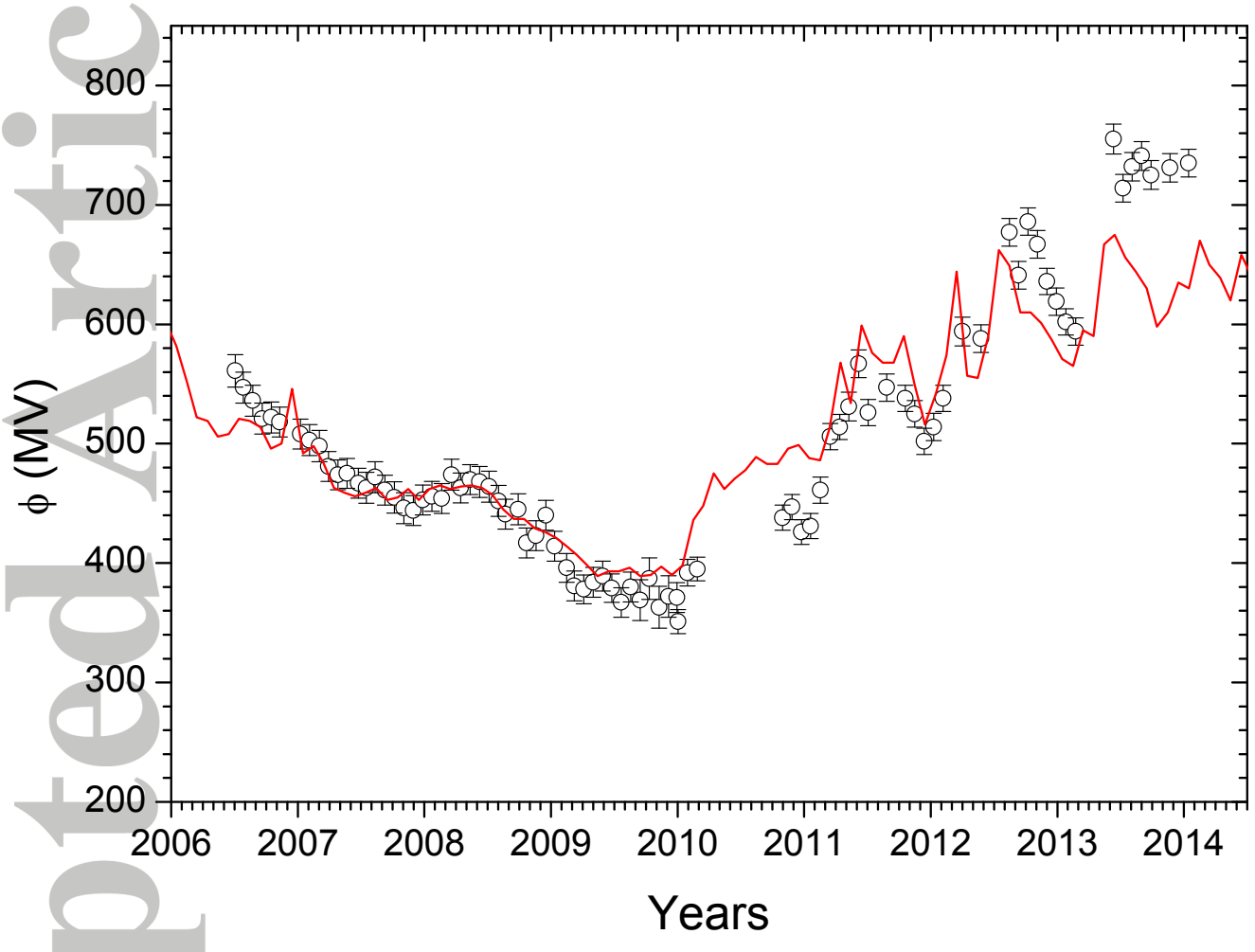

Figure 5. Time profiles of the modulation potential ϕ for the period covered by PAMELA data. Dots with error bars represent the fit to PAMELA data (Table 1), while the red curve is based solely on NM data [*Usoskin et al.*, 2017].